Electronic Materials Letters, Vol. 1, No. 1 (2005), pp. 53-57

Room-Temperature Ferromagnetic Behavior of Homoepitaxial Mn-Doped Si Thin Films Grown by Laser Molecular-Beam Epitaxy

Sug Woo Jung, Gyu-Chul Yi*, Yunki Kim[1], Sunglae Cho[2], and J. F. Webb[3]

National Creative Research Initiative Center for Semiconductor Nanorods and Department of Materials Science and Engineering, Pohang University of Science and Technology (POSTECH), Pohang, Gyeongbuk 790-784, Korea
[1]Department of Electrophysics, Kwangwoon University, Seoul 139-701, Korea
[2]Department of Physics,University of Ulsan, Ulsan 680-749, Korea
[3]School of Mechanical Engineering, Yeungnam University, Gyeongsan, Gyeongbuk 712-749, Korea

We report on the ferromagnetic characteristics of homoepitaxial Mn_xSi_{1-x} ($0.02 \le x \le 0.10$) thin films grown on Si(100) substrates using laser molecular-beam epitaxy. The influence of Mn doping concentration on the structural and magnetic properties of Mn-doped Si thin films was investigated in detail using both synchrotron-radiation x-ray diffraction and a superconducting quantum interference device magnetometer. With the addition of a Mn-Si-related secondary phase, Mn-doped Si thin films showed ferromagnetic behavior above room temperature.

Keywords: Mn_xSi_{1-x} thin film, spintronics, ferromagnetism, homoepitaxy, laser molecular-beam epitaxy

Spintronics has captured the attention of many researchers in recent years. Using both the charge and spin properties of carriers, spintronic devices can be made more functional by combining standard microelectronics with spin-dependent effects allowing for many potential applications.[1, 2] Transition metal (TM) doped semiconductors, which demonstrate room temperature ferromagnetic behavior, are important for the fabrication of spin-controlled electronic devices and integrated magnetic devices. For applications, it is highly desirable to investigate TM doping of the most common semiconductors. In spite of the widespread use of Si and Ge-based electronics, TM doping of group-IV semiconductors has not been attractive, due to the low solubility of TM in these semiconductors as compared to II-VI and III-V semiconductors, such as ZnO, GaN, and GaAs semiconductors[3-5].

Ferromagnetic properties of TM-doped group-IV semiconductors have recently been reported; however, whether these properties originate from secondary phases is still controversial. For example, although Park *et al.*[6] have argued that Mn_xGe_{1-x} thin films grown at low temperature (~300 °C) showed ferromagnetic behavior, the observed behavior may have resulted from $Mn_{11}Ge_8$ secondary phases precipitated in the Ge host matrix. Yokota *et al.*[7] also reported that spin glass behavior appears in Ce-doped Si bulk single crystals with Ce-related secondary phases embedded, such as Ce_5Si_4 and CeSi. Recently, Zhang *et al.*[8] have found that $Mn_{0.05}Si_{0.95}$ thin films showed ferromagnetic behavior above room temperature; however, structural investigations of $Mn_{0.05}Si_{0.95}$ thin films were not carried out in detail. Generally, Mn-rich Si phases would not be easily detected in thin films with conventional x-ray diffraction (XRD) measurements. Therefore, more detailed structural characterizations assisted by synchrotron radiation x-ray diffraction (SR-XRD) and transmission electron microscopy (TEM) should be carried out. In this research paper, we focus on the magnetic and structural properties of Mn_xSi_{1-x} ($0.02 \le x \le 0.10$) thin films with various Mn concentrations.

Mn-doped Si thin films were homoepitaxially grown on Si substrates using laser molecular beam epitaxy (LMBE)[9]. The base pressure of the ultrahigh vacuum chamber was as low as mid-10^{-9} torr. Meanwhile, a polycrystalline Mn-doped Si target was made via the standard arc melting method with a base pressure of 4.0×10^{-7} torr in a high vacuum chamber using Si (99.999%) and Mn (99.999%) powders. We used different Mn concentrations in the Mn_xSi_{1-x} target in the range of 2-10 mol%. The Si substrates were chemically cleaned using standard HF/H_2O etching and H_2O_2/H_2O rinsing solutions. Final cleaning was accomplished by raising the substrate temperature to approximately 750 °C in the LMBE chamber for desorption of the hydrogen passivated layer on the Si substrate, as indicated by *in situ*

*Corresponding author: gcyi@postech.ac.kr

reflection high energy electron diffraction (RHEED). For film growth, the stoichiometric Mn_xSi_{1-x} targets were ablated using the third harmonics of a pulsed Nd:YAG laser. The fluence of the laser beam was 1 J/cm^2. The growth temperature investigated in this research was in the range of 400-700 °C, and the typical film thickness was 1 μm. The compositions of as-grown thin films were measured using induced coupled plasma mass spectroscopy (ICPMS).

The crystal orientation and magnetic properties of the Mn-doped Si thin films were investigated using SR-XRD and a superconducting quantum interference device (SQUID) magnetometer. The SR-XRD measurements were performed using a four-circle diffractometer, which is part of the 3C2 synchrotron x-ray diffraction beam line at the Pohang Light

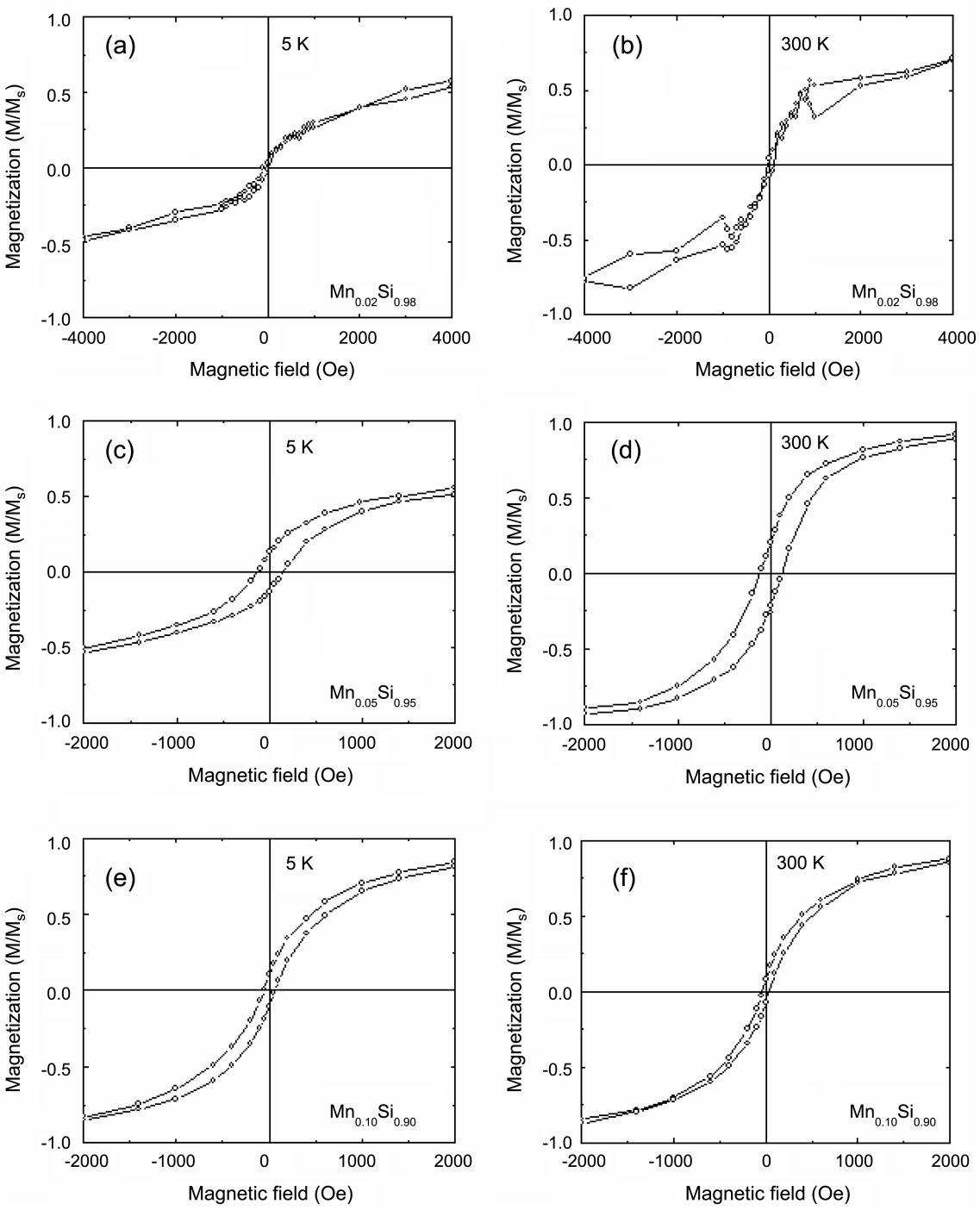

Fig. 1. *M–H* curves of thin films measured at 5 K and room temperature: (a), (b), $Mn_{0.02}Si_{0.98}$; (c), (d), $Mn_{0.05}Si_{0.95}$; and (e), (f), $Mn_{0.10}Si_{0.90}$. Magnetization curves were measured with the applied magnetic field parallel to the surface of the substrate.

Source (PLS). To investigate the magnetic properties of the films, temperature-dependent magnetization (*M-T*) and magnetic hysteresis curves (*M-H*) were measured using a SQUID magnetometer. Both field and temperature-dependent magnetization curves were measured with the applied magnetic field parallel to the surface of the substrate. The *M-T* curves were measured both in zero-field cooled (ZFC) and field-cooled (FC) modes with an applied magnetic field of 100 Oe. The *M-H* curves were measured at 5 K and at room temperature in the range of $-2000 \leq H \leq 2000$. Diamagnetic background from the Si substrates was subtracted for the data presented here.

Figure 1(a) and (b) shows the magnetic hysteresis curves for a $Mn_{0.02}Si_{0.98}$ thin film measured at 5 and 300 K. The magnetization curve has a steep slope below 0.1 T and zero values for M_r and H_c. The *M-H* curve at 300 K did not show any saturation, even at high magnetic fields (~5 T). As will be discussed later, this magnetic behavior presumably results from superparamagnetism. Similar superparamagnetic behavior in Ce-doped Si films has previously been reported by Yokota *et al*.[10]

Furthermore, the *M-H* curves for a $Mn_{0.05}Si_{0.95}$ thin film measured at 5 and 300 K exhibit ferromagnetic behavior, as shown in Fig. 1(c) and (d). The *M-H* curve at 300 K was saturated at 5100 Oe. The H_c and remanence ratio values were 148 Oe and 42.1%, respectively. The *M-H* curve at 5 K showed magnetic saturation at 2 T, and the H_c and remanence ratio values were 146 Oe and 20%, respectively. The observation of a remanence ratio at 5 K that was smaller than that at room temperature suggests that weak non-ferromagnetic ordering appears at low temperatures.[11] Figure 1(e) and (f) show the *M-H* curves for a $Mn_{0.10}Si_{0.90}$ thin film measured at 5 and 300 K. The magnetization for the $Mn_{0.10}Si_{0.90}$ thin film at 300 K was saturated at 5000 Oe. The H_c and remanence ratio values were 37 Oe and 7.9%, respectively. For the *M-H* curve at 5 K, the H_c and remanence ratio values were 58 Oe and 10.3%, respectively. This indicates that a clear hysteresis loop is apparent at room temperature.

The superparamagnetic behavior of the $Mn_{0.02}Si_{0.98}$ thin film observed in Fig. 1(a) and (b) was investigated in detail with magnetic susceptibility measurements. Figure 2(a) shows FC and ZFC magnetization curves for the $Mn_{0.02}Si_{0.98}$ thin film. Magnetization, *M*, as a function of temperature was measured from 5 to 350 K with an applied magnetic field of 100 Oe. The differences between the ZFC and FC values of *M* at different temperatures below 155 K are probably due to spin glass behavior[11], whereas the ZFC and FC values of *M* coincide above 155 K.

In contrast to the $Mn_{0.02}Si_{0.98}$ thin film, the $Mn_{0.05}Si_{0.95}$ thin film shows ferromagnetic behavior at room temperature, as shown in Fig. 2(b). For the FC *M-T* curve, magnetization decreases with increasing temperature up to 66 K; between this temperature and 250 K, it increases slightly and then decreases as the temperature is further increased to 350 K. From this observation, T_c for the $Mn_{0.05}Si_{0.95}$ thin film is esti-

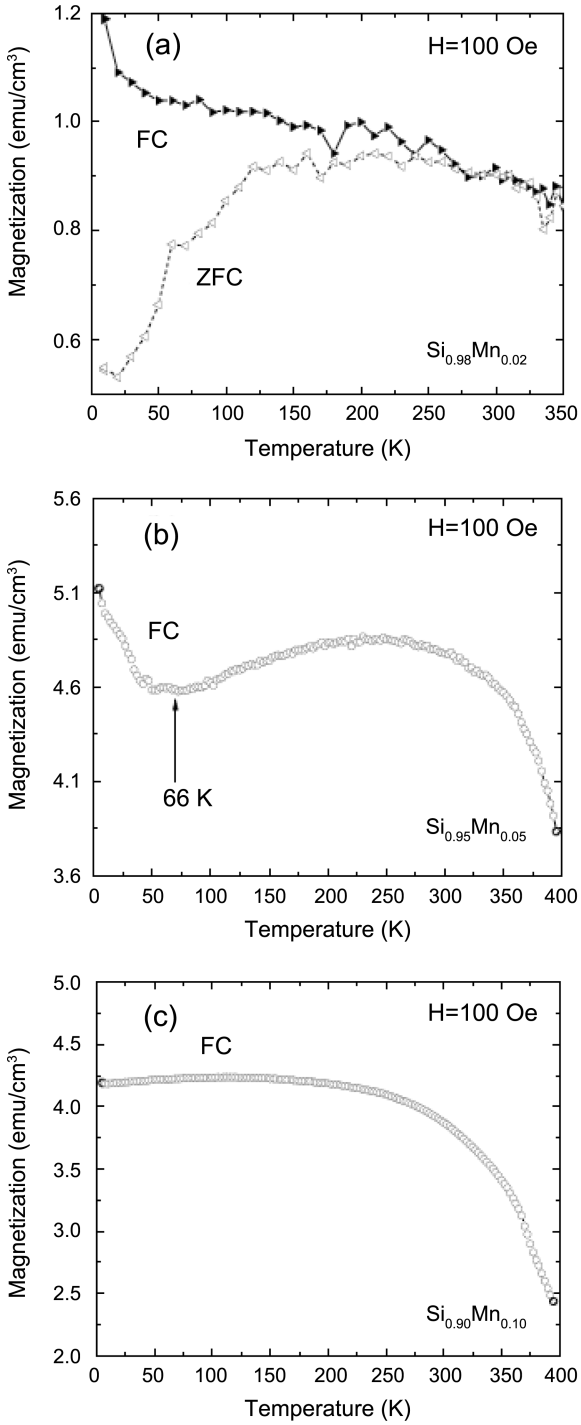

Fig. 2. *M–T* curves measured at a magnetic field of 100 Oe applied parallel to the substrate surface: (a), FC and ZFC magnetization curves as a function of temperature for the $Mn_{0.02}Si_{0.98}$ thin film; (b), FC magnetization curves for the $Mn_{0.05}Si_{0.95}$ thin film; (c), FC magnetization curves for the $Mn_{0.10}Si_{0.90}$ thin film.

mated to be higher than 350 K. However, the distinct slope change at around 66 K indicates that antiferromagnetic components affect the *M-T* curve in the low temperature range. Accordingly, the non-ferromagnetic ordering at low temperatures in Fig. 1(c) may originate from antiferromagnetic components in the Mn-doped Si thin film. This antiferromagnetic component presumably results from the Mn_5Si_3 phase, which has a Néel temperature of 66 K. Meanwhile, as shown in Fig. 2(c), the $Mn_{0.10}Si_{0.90}$ thin film exhibits ferromagnetic behavior in which the Curie temperature is higher than room temperature.

Further attempts were made to identify the secondary phases in Mn_xSi_{1-x} ($0.02 \le x \le 0.10$) by SR-XRD measurements. Figure 3 shows a logarithmic scale SR-XRD θ-2θ scan of a $Mn_{0.02}Si_{0.98}$ homoepitaxially grown thin film on a Si(100) substrate. From the XRD data, only Si related peaks were observed without any significant XRD peaks, due to Mn related secondary phases within the noise signal range of these measurements. As shown in Fig. 3, the strong XRD peak from the Si(100) plane and weak peaks from Si(111), Si(220), and Si(311) planes are also shown at 68.94°, 28.43°, 47.27°, and 56.10°, respectively. However, increasing the Mn concentration up to 5 mol% caused Mn_5Si_2, $Mn_{81.5}Si_{18.5}$, and Mn_5Si_3 related phases to appear abruptly at 26.98°, 32.37°, 33.98°, 46.35°, 53.91°, and 32.12°, in contrast to the $Mn_{0.02}Si_{0.98}$ thin film. The formation of a Mn_5Si_3 phase is consistent with the antiferromagnetic behavior of the $Mn_{0.05}Si_{0.95}$ thin film at low temperatures in Fig. 1(c) and (d).

When increasing the Mn concentration to 10 mol%, dominant XRD peaks were observed at 25.96°, 32.49°, 42.21°, 46.45°, 47.65°, 50.20°, 50.97°, 54.19°, and 54.45°, due to the Si-related phases and phases of Mn abundant silicides, such as Mn_5Si_2 and Mn_5Si_3. This is consistent with a report by Nakayama *et al.*[13] on epitaxial Si thin films heavily doped with Mn, which showed that Mn abundant Mn_5Si_3 phases are formed beyond the Mn solution limit in a Si matrix at close to 10 mol% doping of Mn atoms.

The formation of secondary phases affects the magnetic properties of Mn-doped Si thin films as is evident from the *M-H* curves. It is well known that in Mn-Si systems, ferromagnetic behavior is only exhibited in MnSi intermetallic compounds, which have a T_c of 29 K. Other Mn-Si silicides such as Mn_3Si, Mn_5Si_3, and $Mn_{11}Si_{19}$ indicate antiferromagnetic behavior below 100 K, and Mn_5Si_2 shows non-magnetic behavior[14]. The formation of a Mn-Si secondary phase suggests some kind of inhomogeneity of Mn atoms in the Si matrix. In contrast, Zhang *et al.* have reported that polycrystalline $Mn_{0.05}Si_{0.95}$ thin films grown on Si(100) substrates do not have any secondary phase. Yet, an uncertain peak is visible around 42° in the XRD data compared to the Joint Committee for Powder Diffraction Studies (JCPDS) files. Zhang *et al.* argued that the XRD peak around 42° resulted from Si(210). However, there should be no Si(210) peak originating from the face-centered cubic (FCC) or the hexagonal crystal structure marked around 42°, because the *hkl* parameters of the Si(*hkl*) plane should be either all even or all odd for FCC crystal structures. We presume that the XRD peak around 42° in the previous report by Zhang *et al.* resulted from the Mn_5Si_2(223) peak of a Mn_5Si_2 secondary phase in the film and that the ferromagnetic behavior of the Mn-doped Si films may also be related to a secondary phase which formed in the heavily Mn doped films.

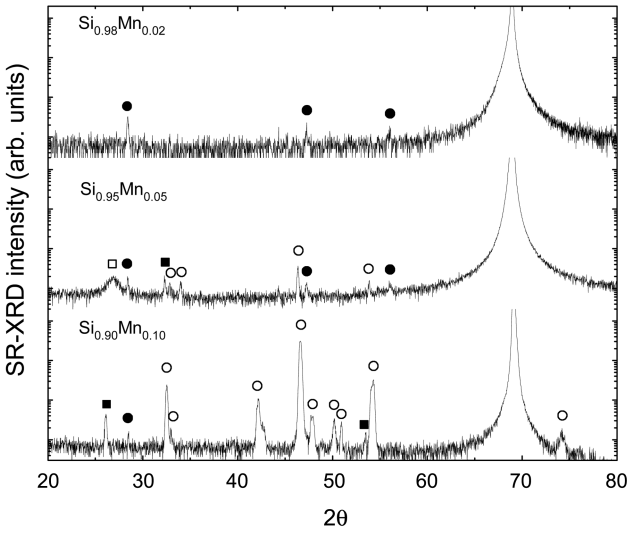

Fig. 3. SR-XRD diffraction patterns of Mn_xSi_{1-x} ($0.02 \le x \le 0.10$) homoepitaxial thin films grown on Si(100) substrate at 700 °C. The large peak belongs to the Si structure, while the small peaks originate from Si (●), and Mn-related secondary phases: Mn_5Si_2 (○), $Mn_{81.5}Si_{18.5}$ (□), and Mn_5Si_3 (■). By increasing Mn concentrations, Mn-rich secondary phases become dominant due to the inhomogeneity of Mn atoms in the thin films.

In conclusion, Mn_xSi_{1-x} ($0.02 \le x \le 0.10$) homoepitaxial films were grown on Si(100) substrates via LMBE. The $Mn_{0.02}Si_{0.98}$ thin film shows superparamagnetic behavior, as demonstrated by the *M-H* and *M-T* curves. However, magnetic hysteresis curves showed (1) that increasing the Mn concentration, first to 5 mol% and then to 10 mol%, causes the Mn-doped Si thin films to become ferromagnetic and (2) that the value of T_c obtained from temperature-dependent magnetization curves was above room temperature. Furthermore, secondary phases were observed even in homoepitaxial films using SR-XRD, which suggests that the ferromagnetic behavior in Mn-doped Si films may be related to Mn rich secondary phases.

ACKNOWLEDGMENTS

This work was supported by the National Creative Research Initiative Project and the Information & Communication Fundamental Technology Research Program (No. 03-Fu-110). One of the authors, J. F. Webb, would like to offer appreciation to the Brain Korea 21 program for funding.

REFERENCES

1. G. A. Prinz, *Science* **282**, 1660 (1998).
2. Y. Ohno, D. K. Young, B. Beschoten, F. Matsukura, H. Ohno, and D. D. Awschalom, *Nature* **402**, 790 (1999).
3. S. W. Jung, S. -J. An, G. -C. Yi, C. U. Jung, S. -I. Lee, and S. Cho, *Appl. Phys. Lett*. **80**, 4561 (2002).
4. H. Ohno, *Science* **281**, 951 (1998).
5. T. Dietl, H. Ohno, F. Matsukura, J. Cibert, and D. Ferrand, *Science* **287**, 1019 (2000).
6. Y. D. Park, A. Wilson, A. T. Hanbicki, J. E. Mattson, T. F. Ambrose, G. Spanos, and B. T. Jonker, *Appl. Phys. Lett.* **78**, 2739 (2001).
7. T. Yokota, N. Fujimura, Y. Morinaga, and T. Ito, *Physica E* **10**, 237 (2001).
8. F. M. Zhang, X. C. Liu, J. Gao, X. S. Wu, Y. W. Du, H. Zhu, J. Q. Xiao, and P. Chen, *Appl. Phys. Lett*. **85**, 786 (2004).
9. S.-J. An, W.I. Park, G.-C. Yi, and S. Cho, *Appl. Phys. A: Mater. Sci. Process.* **74**, 509 (2002).
10. T. Yokota, N. Fujimura, T. Wada, S. Hamasaki, and T. Ito, *J. Appl. Phys.* **91**, 7905 (2002).
11. S. Cho, S. Choi, S.-C. Hong, Y. Kim, J. B. Ketterson, B.-J, Kim, Y. C. Kim, and J.-H. Jung, *Phys. Rev. B*. **66**, 033303 (2002).
12. K. Binder and A. P. Young, *Mod. Phys. Lett. A* **58**, 801 (1986).
13. H. Nakayama, H. Ohta, and E. Kulatov, *Physica B* **302-303**, 419 (2001).
14. K. H. J. Buschow, *Handbook of Magnetic Materials,* Vol. 9. Elsevier Science, Amsterdam (1995).